La Horqueta Formation: Geochemistry, Isotopic Data, and Provenance Analysis

Paulina Abre, Carlos A. Cingolani, Farid Chemale Jr. and Norberto Javier Uriz

Abstract La Horqueta Formation is developed from the Seco de las Peñas River to Agua de la Piedra creek within the San Rafael block and was deposited in a marine environment. It comprises dominantly metasandstones, although metasiltstones, metapelites, and rare metaconglomerates are also present. The base of the succession is not exposed and it is superposed through unconformity by Upper Carboniferous units. La Horqueta Formation is folded and shows cleavage. Provenance analyses based on whole-rock geochemistry and isotope data is the main focus of the work. Whole-rock geochemical data point to a derivation from unrecycled upper continental crust, based mainly on Th/Sc, Zr/Sc, La/Th, and Th/U ratios and rare earth element (REE) patterns (including Eu anomalies). Sc, Cr, and V concentrations and low Th/Sc ratios are indicative of a source slightly less evolved than the average upper continental crust. The εNd values are within the range of variation of data from the Mesoproterozoic Cerro La Ventana Formation, which is part of the basement of the Cuyania terrane outcropping within the San Rafael block. The Rb-Sr whole-rock data indicate that the low-grade metamorphism and folding events are Devonian in age. U-Pb detrital zircon ages suggest main derivation from the Mesoproterozoic ("Grenvillian-age") basement of the San

P. Abre (✉)
Centro Universitario de la Región Este, Universidad de la República,
Ruta 8 Km 282, Treinta y Tres, Uruguay
e-mail: paulinabre@yahoo.com.ar

C.A. Cingolani
Centro de Investigaciones Geológicas, CONICET-Universidad Nacional de La Plata,
Calle 1 no. 644, B1900TAC La Plata, Argentina
e-mail: carloscingolani@yahoo.com

C.A. Cingolani · N.J. Uriz
División Geología, Museo de La Plata, Universidad Nacional de La Plata,
Paseo del Bosque s/n, La Plata, Argentina
e-mail: norjuz@gmail.com

F. Chemale Jr.
Programa de Pós-Graduação Em Geologia, Universidade Do Vale Do Rio Dos Sinos,
São Leopoldo RS, Brazil
e-mail: faridchemale@gmail.com

C.A. Cingolani (ed.), *Pre-Carboniferous Evolution of the San Rafael Block, Argentina*, Springer Earth System Sciences,
DOI 10.1007/978-3-319-50153-6_9

Rafael block and the Pampean–Brasiliano cycle, as well as a detrital input from the Río de la Plata craton and the Famatinian belt. Despite geochemical similarities, Río Seco de los Castaños Formation display different proportions of detrital zircon ages, when compared to La Horqueta Formation.

Keywords Geochemistry · Isotope data · Provenance · La Horqueta Formation · San Rafael Block · Cuyania terrane

1 Introduction and Geological Setting

La Horqueta Formation (Dessanti 1956; González Díaz 1981) crops out on a 12 km-wide strip developed from the Seco de las Peñas River to Agua de la Piedra creek (Fig. 1; Cuerda and Cingolani 1998; Cingolani et al. 2003a), within the San Rafael block. It is in tectonic contact with Carboniferous units, either by reverse faults or by an angular unconformity (Tickyj et al. this volume).

La Horqueta Formation was deposited in a marine environment and comprises dominantly metasandstones, although metasiltstones, metapelites, and rare metaconglomerates are also present. The matrix of the metasandstones was recrystallized into chlorite, illite, quartz, albite, and minor smectite. Foliation is penetrative in some layers; ductile deformed clasts are present as well as pseudomatrix. In less-deformed metawackes, the relictic clasts are mainly composed of monocrystalline and polycrystalline quartz, sedimentary and metasedimentary lithoclasts, with scarce volcanic and limestone lithoclasts, and rare feldspars. The fine-grained levels are metamorphosed to phyllites and they comprise oriented illite and chlorite with scarce quartz and feldspar grains (Tickyj et al. this volume). In several outcrops quartz veins cutting the La Horqueta unit are conspicuous (Fig. 2c, d, e). Toward north, (Los Gateados river; Fig. 1) the unit consists of muscovite–biotite schists interlayered with quartzitic schists showing granolepidoblastic textures.

The base of the succession is not exposed and it is overlaid through unconformity by the Upper Carboniferous marine-glacial-continental unit (El Imperial Formation). La Horqueta Formation was affected by deformational events; it is folded and develops cleavage. The regional metamorphic conditions slightly increase from south to north (Criado Roqué 1972; Criado Roqué and Ibáñez 1979), ranging from very low (anchizone) to low grade (epizone). Maximum Silurian–Devonian depositional age was determined using U-Pb detrital zircon dating (Cingolani et al. 2008; Tickyj et al. this volume).

La Horqueta Formation is intruded by a granitic stock known as Agua de la Chilena, which extends over 5 km^2 of the northwestern part of the San Rafael Block and it is covered by Quaternary volcanic rocks (Cingolani et al. 2005a). The stock is composed of diorites, tonalites and biotitic-horblendiferous, and leucocratic granodiorites; grain size is medium to fine. Xenoliths and enclaves are frequent. Their mineralogical constituents are subhedral to anhedral quartz (27–33%), subhedral to euhedral altered alkaline feldspars (10–20%) and plagioclases (51–59%)

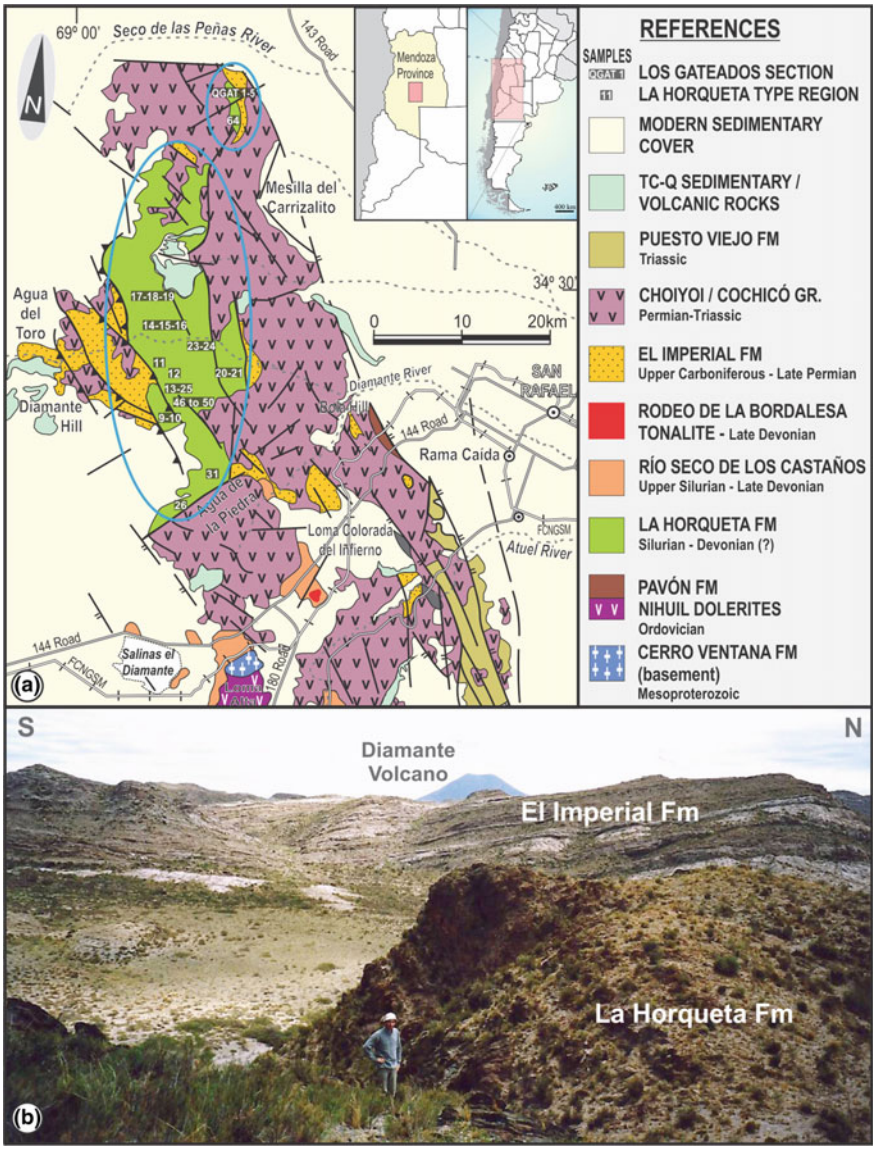

Fig. 1 **a** Geological sketch map of the studied area within the San Rafael block, where outcrops and sampling zone of La Horqueta Formation are located northward. **b** Regional view toward the West near La Horqueta type area. It is shown the deformed outcrops of La Horqueta Fm superposed by the *Upper* Paleozoic El Imperial Fm. The Quaternary Diamante Volcano is also shown

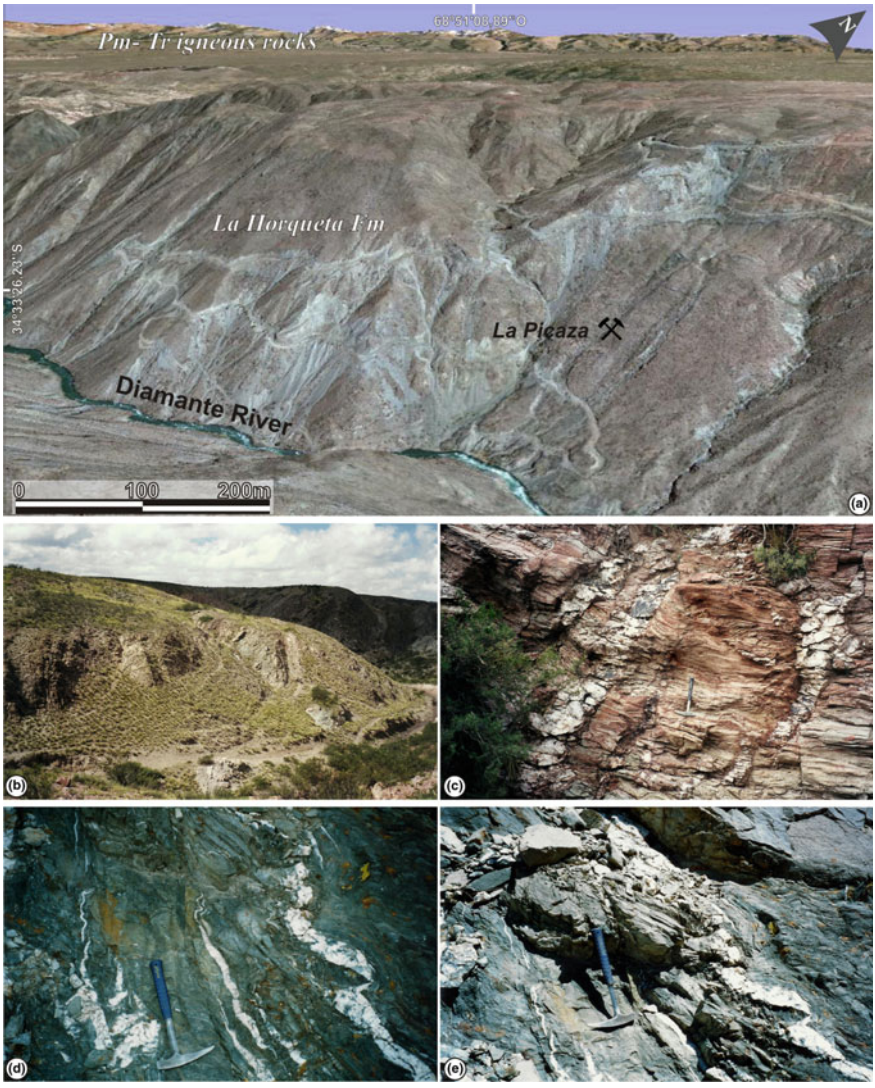

Fig. 2 **a** Google satellite image around Diamante river type section, within the area of the La Picaza old mine and Agua de la Chilena. **b** Outcrops of La Horqueta Formation at Agua de la Piedra section. **c**, **d**, **e** Some details of abundant quartz veins crosscutting folded layers of La Horqueta Formation at Agua de la Chilena and Agua de la Piedra outcrops

as well as biotite, amphiboles, and epidotes. Accessory minerals are apatite and zircon, and scarce titanite. The texture is granular hypidiomorphic and locally pegmatitic.

The stock was dated using the Rb-Sr method on whole rock and biotite on one sample, giving an age of 256 ± 2 Ma, with a Ri = 0.7073 ± 0.0001. However, a

more accurate age is obtained combining whole-rock Rb-Sr of five samples with data from feldspars and biotite, which assigned a Guadalupian–Lopingian age of 257 ± 3 Ma, with a Ri = 0.7069 ± 0.0003 and MSWD of 8.6 following ISOPLOT model 3. The stock would have been emplaced after the Orogenic San Rafael Phase (Asselian—Sakmarian), and during the latest stages of volcanic activity linked to the Cochicó Group (Cingolani et al. 2005a). Based on the presence of amphibole together with biotite a metaluminous series with calcoalcaline characteristics can be assumed, which are typical of magmatic arcs related to the subduction of the paleopacific plate within the southwestern margin of Gondwana. This Permian magmatism could have originated the mineralization of El Rodeo and Las Picazas sulfides mines (arsenopyrite, pyrite and sphalerite), as well as the hydrothermal hematite of the Alto Molle mine (within the La Horqueta Formation; (Cingolani et al. 2005a).

The present work focus on provenance analyses of La Horqueta Formation based on whole-rock geochemistry and Sm–Nd data, which altogether with the information presented in Tickyj et al. (this volume), particularly regarding detrital zircon dating and Rb-Sr whole-rock data, give insights into source composition and the comparison with Río Seco de los Castaños Formation.

2 Sampling and Analytical Techniques

Sampling was done (see Tickyj et al. this volume) at Los Gateados and La Horqueta type areas (Fig. 1 and Table 1). A total of eighteen samples were selected for chemical analyses done at ACME Labs, Canada. Major elements were obtained by inductively coupled plasma element spectroscopy (ICP-ES) on fusion beads and the loss on ignition (LOI) was calculated by weight after ignition at 1000 °C. Mo, Cu, Pb, Zn, Ni, As, Cd, Sb, Bi, Ag, Au, Hg, Tl, and Se were analyzed by inductively coupled plasma mass spectroscopy (ICP-MS) after leaching each sample with 3 ml 2:2:2 HCl–HNO_3–H_2O at 95 °C for 1 hour and later diluted to 10 ml. Rare earth elements (REE) and certain trace elements (Ba, Be, Co, Cs, Ga, Hf, Nb, Rb, Sn, Sr, Ta, Sc, Th, U, V, W, Zr, Y, La, Ce, Pr, Nd, Sm, Eu, Gd, Tb, Dy, Ho, Er, Tm, Yb, Lu) were analyzed by ICP-MS following lithium metaborate/tetraborate fusion and nitric acid digestion. Detection limits are: 0.01% for major elements, except for Fe_2O_3 which is 0.04%; 0.1 ppm for Mo, Cu, Pb, Cd, Sb, Bi, Ag, Tl, Cs, Hf, Nb, Rb, Ta, U, Zr, Y, La, and Ce; 1 ppm for Zn, Ba, Be, Sn, and Sc; 0.5 ppm for As, Au, Ga, Sr, and W; 0.01 ppm for Hg, Tm, Lu, and Tb; 0.2 ppm for Co and Th; 8 ppm for V; 20 ppm for Ni; 0.002 ppm for Cr; 0.02 ppm for Pr, Eu, and Ho; 0.3 ppm for Nd; 0.05 ppm for Sm, Gd, Dy, and Yb and 0.03 ppm for Er. Data are presented in Tables 2, 3, 4 and 5.

Seven whole-rock samples were used for Sm–Nd determinations; they were spiked with mixed ^{149}Sm–^{150}Nd tracer and dissolved in Teflon vial using an HF–HNO_3 mixture and 6 N HCl until complete material dissolution. The cationic resin AG-50 W-X8 (200–400 mesh) were used for column separation of the REE,

Table 1 GPS location of studied samples (after Tickyj et al,. this volume)

Sample	Location
Hor 9	34° 38′ 16.53″S–68° 53′ 11.11″W
Hor 10	34° 38′ 16.53″S–68° 53′ 11.11″W
Hor 11	34° 33′ 57.64″S–68° 54′ 05.05″W
Hor 14	34° 33′ 02.56″S–68° 51′ 04.83″W
Hor 15	34° 33′ 02.56″S–68° 51′ 04.83″W
Hor 16	34° 33′ 02.56″S–68° 51′ 04.83″W
Hor 17	34° 30′ 04.40″S–68° 55′ 07.01″W
Hor 18	34° 30′ 04.40″S–68° 55′ 07.01″W
Hor 20	34° 34′ 25.96″S–68° 46′ 40.08″W
Hor 21	34° 34′ 25.96″S–68° 46′ 40.08″W
Hor 24	34° 33′ 53.22″S–68° 49′ 35.48″W
Hor 27	34° 44′ 31.69″S–68° 49′ 34.90″W
Hor 64	34° 17′ 24.00″S–68° 48′ 49.57″W
Hor 50	34° 38′ 08.78″S–68° 48′ 49.57″W
Hor 53	34° 38′ 08.78″S–68° 48′ 9.57″W
Hor 66	34° 35′ 48.00″S–68° 52′ 32.00″W
Hor 67	34° 35′ 48.00″S–68° 52′ 32.00″W
QGAT1	34° 17′ 24.00″S–68° 48′ 49.57″W
QGAT2	34° 17′ 24.00″S–68° 48′ 49.57″W
QGAT3	34° 17′ 24.00″S–68° 48′ 49.57″W
QGAT4	34° 17′ 24.00″S–68° 48′ 49.57″W
QGAT5	34° 17′ 24.00″S–68° 48′ 49.57″W

followed by Sm and Nd separation using anionic politeflon HDEHP LN-B50-A (100–200 μm) resin according to Patchett and Ruiz (1987). Each sample was dried to a solid and then loaded with 0.25 N H_3PO_4 on appropriated filament (single Ta for Sm and triple Ta–Re–Ta for Nd). Isotopic ratios were measured in static mode with a VG Sector 54 multicollector mass spectrometer at the Laboratorio de Geología Isotópica, Universidade Federal do Rio Grande do Sul (LGI-UFRGS, Porto Alegre, Brazil). 100–120 ratios with a 0.5–1 V ^{144}Nd beam were normally collected. Nd ratios were normalized to $^{146}Nd/^{144}Nd = 0.72190$. All analyses were adjusted for variations instrumental bias due to periodic adjustment of collector positions as monitored by measurements of our internal standards. Measurements for the Spex $^{143}Nd/^{144}Nd$ are 0.511130 ± 0.000010. Correction for blank was insignificant for Nd isotopic compositions and generally insignificant for Sm/Nd ratios. $f_{Sm/Nd}$ is the fractional deviation of the sample $^{147}Sm/^{144}Nd$ from achondritic reference and is calculated as $(^{147}Sm/^{144}Nd)_{sample}/(^{147}Sm/^{144}Nd)_{CHUR} - 1$. The εNd indicates the deviation of the $^{143}Nd/^{144}Nd$ value of the sample from that of CHUR (DePaolo and Wasserburg 1976) and it is calculated as $\varepsilon Nd_{(0)} = \{[(^{143}Nd/^{144}Nd)_{sample(t=0)}/0.512638] - 1\} * 10{,}000$, whereas $\varepsilon Nd_{(t=420\ Ma)} = \{[(^{143}Nd/^{144}Nd)_{sample\ (t)}/(^{143}Nd/^{144}Nd)_{CHUR\ (t)}] - 1\} * 10{,}000$. Parameters used are: $(^{147}Sm/^{144}Nd)_{CHUR} = 0.1967$. $(^{143}Nd/^{144}Nd)_{CHUR} = 0.512638$. T_{DM}

Table 2 Major elements (expressed in %) of La Horqueta Formation

	HOR 1O	HOR 15	HOR 21	HOR 27	HOR 9	HOR 11	HOR 14	HOR 16	HOR 17	HOR 24	HOR 18	HOR 20	HOR 64	QGAT1	QGAT2	QGAT3	QGAT4	QGAT5	Average
SiO_2	67.85	70.28	69.32	65.23	59.26	52.50	58.79	58.39	49.97	44.69	52.79	45.48	66.27	77.45	76.78	76.71	78.19	83.17	64.06
Al_2O_3	13.62	12.51	12.54	15.43	18.09	21.89	19.78	20.43	24.46	24.48	22.36	24.35	15.48	9.78	10.32	10.45	9.94	7.32	16.29
Fe_2O_3	7.27	6.98	6.95	2.43	8.50	7.77	6.86	6.29	7.21	10.89	7.16	9.19	5.72	4.43	4.51	4.47	4.11	3.33	6.34
MnO	0.07	0.05	0.04	0.02	0.07	0.07	0.04	0.04	0.03	0.10	0.03	0.09	0.04	0.04	0.04	0.04	0.04	0.03	0.05
MgO	2.26	2.30	2.63	1.48	2.62	3.10	2.33	2.19	2.87	5.11	2.70	3.74	1.85	1.52	1.53	1.49	1.27	1.09	2.34
CaO	0.78	0.39	0.60	2.62	0.25	0.47	0.22	0.28	0.29	0.34	0.62	1.56	0.31	0.44	0.39	0.35	0.39	0.30	0.59
Na_2O	1.63	1.63	1.38	2.78	1.40	1.90	1.37	1.04	0.77	0.08	0.66	0.56	1.81	2.16	1.92	1.91	1.97	1.55	1.47
K_2O	2.14	1.86	1.89	2.87	3.51	5.36	4.85	5.59	6.84	5.92	6.01	5.82	3.30	1.71	1.90	2.01	1.72	1.23	3.59
TiO_2	1.06	1.05	1.12	0.74	0.99	1.07	0.86	0.96	1.09	1.20	1.05	1.16	0.83	0.69	0.66	0.65	0.62	0.46	0.90
P_2O_5	0.25	0.20	0.19	0.12	0.16	0.33	0.18	0.17	0.18	0.22	0.39	0.32	0.19	0.20	0.18	0.19	0.17	0.18	0.21
LOI	3.49	3.04	3.39	5.65	4.39	4.13	3.53	3.97	4.99	5.80	4.97	6.45	2.83	1.94	2.11	2.04	1.94	1.54	3.68
TOTAL	100.40	100.29	100.05	99.38	99.24	98.60	98.82	99.36	98.69	98.83	98.73	98.72	98.64	100.36	100.34	100.32	100.37	100.20	99.52
CIA	68	70	70	55	73	69	71	71	73	77	72	71	69	61	64	64	63	62	68

Table 3 Trace elements (expressed in ppm) of La Horqueta Formation

	HOR 10	HOR 15	HOR 21	HOR 27	HOR 9	HOR 11	HOR 14	HOR 16	HOR 17	HOR 24	HOR 18	HOR 20	HOR 64	QGAT1	QGAT2	QGAT3	QGAT4	QGAT5	AVERAGE
Sc	18	16	17	7	20	25	20	21	29	31	26	29	17	11	11	15	8	8	18
Be	2	2	2	2	3	4	4	4	5	5	4	4	3	2	2	3	b.d.l.	2	3
V	141	116	140	69	147	219	155	165	218	206	205	212	132	91	89	107	67	65	141
Cr	124	231	178	36	122	136	109	144	127	142	124	145	74	79	60	57	54	51	111
Co	32	32	26	11	28	25	18	19	17	29	15	13	32	45	43	44	55	66	31
Ni	49	83	64	b.d.l.	51	54	36	37	37	82	32	29	71	34	34	36	38	44	48
Cu	62	44	27	15	12	56	34	32	11	56	22	46	31	17	34	22	19	15	31
Zn	126	64	b.d.l.	b.d.l.	94	36	b.d.l.	35	74	91	47	b.d.l.	93	61	61	55	46	41	66
Ga	20	21	16	18	29	30	26	42	39	35	33	29	21	13	13	13	13	9	23
Ge	2	3	2	b.d.l.	5	5	4	6	5	4	4	b.d.l.	2	2	2	2	2	2	3
As	8	43	36	9	b.d.l.	8	17	9	8	29	16	22	15	9	19	6	10	b.d.l.	16
Rb	97	108	128	127	176	250	230	359	338	253	292	277	158	72	79	81	66	56	175
Sr	64	43	54	125	121	50	40	63	46	28	85	97	76	81	62	57	60	52	67
Y	35	51	39	9	48	57	46	66	48	41	58	61	38	29	28	31	27	25	41
Zr	270	325	242	205	213	138	150	264	180	162	153	203	252	377	266	297	293	306	239
Nb	17	23	15	12	21	22	20	30	25	22	22	22	18	11	11	11	11	9	18
Sn	3	3	2	1	3	5	5	7	7	5	5	3	3	1	2	2	1	1	3
Sb	1	1	1	1	1	2	2	2	2	2	2	1	1	0	0	0	0	0	1
Cs	4	7	8	6	8	11	10	17	16	10	14	12	9	4	4	5	4	3	8
Ba	543	360	397	588	691	895	634	938	1070	1020	975	1120	454	214	235	290	207	139	598
Hf	7	9	7	6	6	4	4	8	5	5	5	6	7	10	7	8	8	8	7
Ta	2	2	2	1	2	2	2	3	2	2	2	2	3	3	4	4	4	5	3
W	116	145	111	64	37	17	31	43	14	10	33	31	208	424	503	498	659	792	208

(continued)

Table 3 (continued)

	HOR 10	HOR 15	HOR 21	HOR 27	HOR 9	HOR 11	HOR 14	HOR 16	HOR 17	HOR 24	HOR 18	HOR 20	HOR 64	QGAT1	QGAT2	QGAT3	QGAT4	QGAT5	AVERAGE
Tl	0	0	b.d.l.	b.d.l.	0	0	0	0	1	0	1	0	1	0	0	1	0	0	0
Pb	19	7	b.d.l.	b.d.l.	b.d.l.	b.d.l.	b.d.l.	b.d.l.	b.d.l.	5	b.d.l.	5	8	6	6	6	16	11	9
Bi	1	b.d.l.	b.d.l.	b.d.l.	b.d.l.	b.d.l.	b.d.l.	b.d.l.	0	0	0	b.d.l.	0	b.d.l.	b.d.l.	0	0	0	0
Th	9	12	9	15	17	16	15	26	23	15	18	19	16	12	11	11	11	9	14
U	3	3	3	4	3	5	5	7	4	3	5	4	4	3	3	4	3	3	4

b.d.l below detection limit

Table 4 Rare earth elements (expressed in ppm) of La Horqueta Formation

	HOR 10	HOR 15	HOR 21	HOR 27	HOR 9	HOR 11	HOR 14	HOR 16	HOR 17	HOR 24	HOR 18	HOR 20	HOR 64	QGAT1	QGAT2	QGAT3	QGAT4	QGAT5	Average
La	33.55	43.45	34.57	48.46	61.74	76.61	57.84	84.84	74.83	45.56	66.25	71.46	47.10	32.34	33.05	32.99	32.07	25.99	50.15
Ce	69.85	90.50	72.61	99.48	124.30	143.01	115.77	167.84	151.60	93.20	134.80	145.83	96.10	69.05	67.60	68.73	67.76	54.79	101.82
Pr	8.09	10.27	8.27	11.17	13.72	15.59	12.73	18.34	16.95	10.37	15.34	16.26	11.10	7.68	7.71	7.68	7.72	6.09	11.39
Nd	33.52	42.51	34.43	45.28	53.66	63.24	50.38	72.11	66.46	40.64	63.43	65.45	42.10	29.00	29.51	29.39	28.55	23.17	45.16
Sm	7.12	8.95	7.07	8.10	9.96	12.05	9.57	13.56	10.79	8.02	14.59	12.53	8.40	6.27	6.27	6.31	5.74	5.03	8.91
Eu	1.61	2.01	1.70	1.71	2.02	2.63	1.92	2.79	2.37	1.28	2.69	2.70	1.58	1.24	1.19	1.19	1.16	0.99	1.82
Gd	6.84	9.30	7.20	5.02	9.28	11.42	8.77	12.40	9.33	7.43	13.43	11.66	7.24	5.54	5.09	5.48	5.16	4.38	8.05
Tb	1.13	1.63	1.19	0.46	1.50	1.74	1.40	2.00	1.42	1.29	2.01	1.84	1.21	0.96	0.87	0.94	0.85	0.77	1.29
Dy	6.21	9.23	6.77	1.83	8.21	9.61	7.86	11.17	8.04	7.36	10.45	10.22	6.93	5.57	5.04	5.14	4.85	4.29	7.15
Ho	1.22	1.80	1.35	0.28	1.67	1.93	1.57	2.22	1.64	1.47	1.95	2.08	1.44	1.13	1.03	1.04	1.03	0.86	1.43
Er	3.69	5.26	4.17	0.70	5.21	5.86	4.82	6.85	5.11	4.67	5.80	6.32	4.32	3.21	3.03	3.04	2.90	2.56	4.31
Tm	0.54	0.75	0.59	0.08	0.77	0.82	0.70	1,01	0.77	0.71	0.83	0.91	0.65	0.49	0.46	0.48	0.43	0.39	0.63
Yb	3.41	4.33	3.78	0.48	4.68	4.99	4.29	6.17	4.82	4.36	4.98	5.73	4.05	3.07	2.87	2.94	2.85	2.47	3.90
Lu	0.51	0.59	0.53	0.06	0.70	0.72	0.63	0.92	0.71	0.67	0.69	0.83	0.57	0.45	0.42	0.41	0.42	0.37	0.57
Σ	177.28	230.57	184.24	223.11	297.40	350.20	278.26	402.22	354.85	227.02	337.23	353.82	232.80	165.99	164.14	165.75	161.50	132.15	246.59

Table 5 Selected ratios of La Horqueta Formation

	HOR 10	HOR 15	HOR 21	HOR 27	HOR 9	HOR 11	HOR 14	HOR 16	HOR 17	HOR 24	HOR 18	HOR 20	HOR 64	QGAT1	QGAT2	QGAT3	QGAT4	QGAT5	Average
K/Rb	0.02	0.02	0.01	0.02	0.02	0.02	0.02	0.02	0.02	0.02	0.02	0.02	0.02	0.02	0.02	0.02	0.03	0.02	0.02
Rb/Sr	1.53	2.52	2.36	1.02	1.46	5.04	5.70	5.69	7.35	9.13	3.42	2.85	2.08	0.89	1.27	1.42	1.09	1.08	3.10
Ba/Rb	5.59	3.33	3.10	4.62	3.92	3.58	2.76	2.62	3.17	4.03	3.34	4.04	2.87	2.98	3.00	3.57	3.14	2.47	3.45
Ba/Sr	8.53	8.39	7.31	4.72	5.70	18.01	15.73	14.87	23.27	36.81	11.41	11.53	5.97	2.65	3.81	5.05	3.43	2.66	10.55
Th/U	3.24	3.49	3.46	3.99	5.66	3.25	3.02	3.84	5.34	4.48	3.55	4.98	4.24	3.61	3.45	3.06	3.68	3.42	3.88
Th/Sc	0.51	0.73	0.52	2.07	0.87	0.62	0.76	1.22	0.78	0.50	0.68	0.65	0.94	1.06	1.00	0.74	1.36	1.12	0.90
Zr/Sc	15.03	20.34	14.22	29.31	10.63	5.52	7.48	12.58	6.20	5.22	5.90	7.00	14.82	34.28	24.18	19.81	36.64	38.19	17.07
Zr/Hf	37.80	36.34	35.04	36.98	35.18	32.01	33.59	34.05	33.08	33.29	33.89	34.12	35.00	39.49	36.75	39.33	38.80	39.58	35.79
Zr/Nb	15.93	14.17	15.85	16.60	9.97	6.25	7.46	8.76	7.25	7.34	6.93	9.43	13.77	34.98	24.55	27.58	27.50	33.37	15.98
Zr/Y	7.84	6.38	6.23	22.66	4.39	2.42	3.27	4.01	3.78	3.99	2.64	3.33	6.72	13.11	9.54	9.57	10.69	12.41	7.39
Ti/Zr	23.52	19.29	27.72	21.50	27.84	46.39	34.61	21.82	36.30	44.25	41.05	34.30	19.63	10.94	14.83	13.13	12.74	9.06	25.50
Ti/Nb	374.69	273.24	439.51	357.04	277.71	290.06	258.04	191.11	263.17	324.76	284.27	323.57	270.27	382.65	364.17	362.23	350.46	302.48	316.08
Cr/Zr	0.46	0.71	0.73	0.17	0.57	0.99	0.73	0.55	0.71	0.88	0.81	0.71	0.29	0.21	0.23	0.19	0.18	0.17	0.52
Cr/V	0.88	2.00	1.27	0.52	0.83	0.62	0.70	0.87	0.58	0.69	0.60	0.68	0.56	0.87	0.67	0.53	0.80	0.78	0.80
Cr/Ni	2.54	2.78	2.78		2.37	2.53	3.01	3.86	3.45	1.74	3.92	4.94	1.04	2.29	1.78	1.61	1.43	1.15	2.54
Y/Ni	0.71	0.61	0.61		0.94	1.06	1.27	1.76	1.29	0.50	1.84	2.09	0.53	0.84	0.83	0.87	0.73	0.56	1.00
Sc/Cr	0.15	0.07	0.10	0.20	0.16	0.18	0.18	0.15	0.23	0.22	0.21	0.20	0.23	0.14	0.18	0.26	0.15	0.16	0.18
V/Ni	2.90	1.39	2.19		2.86	4.06	4.30	4.41	5.92	2.52	6.50	7.25	1.86	2.64	2.64	3,01	1.78	1.47	3.39
Ni/Co	1.53	2.58	2.45		1.86	2.19	2.00	2.00	2.13	2.85	2.09	2.20	2.22	0.77	0.78	0.81	0.69	0.68	1.75
La/Th	3.64	3.70	3.93	3.34	3.54	4.93	3.82	3.30	3.30	2.95	3.72	3.81	2.94	2.78	3.01	2.97	2.95	2.89	3.42
La/Sc	1.86	2.72	2.03	6.92	3.09	3.06	2.89	4.04	2.58	1.47	2.55	2.46	2.77	2.94	3.00	2.20	4.01	3.25	2.99
La/Y	0.97	0.85	0.89	5.35	1.28	1.34	1.26	1.29	1.58	1.12	1.14	1.17	1.26	1.12	1.19	1.06	1.17	1.06	1.39

(continued)

Table 5 (continued)

	HOR 10	HOR 15	HOR 21	HOR 27	HOR 9	HOR 11	HOR 14	HOR 16	HOR 17	HOR 24	HOR 18	HOR 20	HOR 64	QGAT1	QGAT2	QGAT3	QGAT4	QGAT5	Average
La/Yb	9.83	10.04	9.15	100.88	13.19	15.36	13.47	13.75	15.52	10.44	13.30	12.46	11.63	10.53	11.50	11.22	11.25	10.52	16.89
La_N/Yb_N	6.64	6.78	6.18	68.17	8.92	10.38	9.10	9.29	10.49	7.05	8.99	8.42	7.86	7.12	7.77	7.58	7.60	7.11	11.41
La_N/Sm_N	2.97	3.05	3.08	3.76	3.90	4.00	3.80	3.94	4.37	3.58	2.86	3.59	3.53	3.25	3.32	3.29	3.52	3.25	3.50
Gd_N/Yb_N	1.62	1.74	1.55	8.47	1.61	1.86	1.66	1.63	1.57	1.38	2.18	1.65	1.45	1.46	1.43	1.51	1.47	1.44	1.98
Eu_N/Eu*	0.70	0.67	0.73	0.82	0.64	0.68	0.64	0.66	0.72	0.51	0.59	0.68	0.62	0.64	0.65	0.62	0.65	0.65	0.66
Sm/Nd	0.21	0.21	0.21	0.18	0.19	0.19	0.19	0.19	0.16	0.20	0.23	0.19	0.20	022	0.21	0.21	0.20	0.22	0.20

Table 6 Sm–Nd data of La Horqueta Formation

Sample	Sm (ppm)	Nd (ppm)	$^{147}Sm/^{144}Nd$	$^{143}Nd/^{144}Nd$	$\varepsilon Nd_{(0)}$	$\varepsilon Nd_{(t)}$	T^1_{DM} (Ga)	T^2_{DM} (Ga)	$f_{(Sm/Nd)}$
Hor 9	6.39	34.56	0.1119	0.512070	−11.07	−6.53	1.45	1.66	−0.43
Hor 10	5.52	26.07	0.1281	0.512192	−8.69	−5.01	1.50	1.55	−0.35
Hor 21	5.07	24.84	0.1233	0.512224	−8.07	−4.14	1.37	1.49	−0.37
Hor 50	4.75	23.35	0.123 1	0.512329	−6.02	−2.07	1.20	1.33	−0.37
Hor 53	7.41	36.77	0.1219	0.512247	−7.63	−3.62	1.31	1.45	−0.38
Hor 66	5.72	27.23	0.1269	0.512253	−7.50	−3.76	1.38	1.46	−0.35
Hor 67	5.64	27.07	0.1259	0.512367	−5.28	−1.49	1.17	1.28	−0.36

T^1_{DM} = DePaolo et al. (1981); T^2_{DM} = DePaolo et al. (1991)

(model ages) were calculated based on the depleted mantle model (DePaolo 1981) and on the three-stage model (DePaolo et al. 1991), as indicated in Table 6.

3 Whole-Rock Geochemistry

Data are presented in Tables 2, 3, 4, and 5. The use of whole-rock geochemistry to described provenance composition has been proven to be useful in the context of the pre-Carboniferous clastic units of the San Rafael block of the Cuyania terrane, as demonstrated by Cingolani et al. (2003b), Manassero et al. (2009), and Abre et al. (2011). Therefore, despite the remobilization that could have occurred due to low-grade metamorphism, it is expected that geochemical proxies using trace and REE of La Horqueta Formation would still reflect source compositions.

In the description of the geochemical proxies that follows, the sample HOR27 is treated separately due to their unique characteristics with respect to the whole dataset. A comparison to Río Seco de los Castaños Formation is introduced, since both units of the San Rafael block show similarities.

La Horqueta Formation shows SiO_2 concentrations ranging from 44.69 to 83.17%, Al_2O_3 is between 7.32 and 24.48%, Fe_2O_3 ranges from 3.33 to 10.89%, CaO is present in low concentrations (0.59% on average), Na_2O contents ranges from 0.08 to 2.16%, whereas K_2O is between 1.23 and 6.84% (Table 2). Sample HOR27 has SiO_2, Al_2O_3, and K_2O in the range of variation of the unit, but has lower Fe_2O_3 (2.43%), and higher CaO and Na_2O contents (2.63 and 2.68%, respectively). Some of the quartz veins cutting La Horqueta Formation were also analyzed for Ag and Au with negative results.

Weathering: The Chemical Index of Alteration (CIA; Nesbitt and Young 1982) is used to evaluate the extent of primary material transformation caused by weathering. The index is calculated using mole fractions as follows: $CIA = \{Al_2O_3/(Al_2O_3 + CaO^* + Na_2O + K_2O)\} \times 100$, where CaO* refers to the calcium associated with silicate minerals.

For La Horqueta Formation, values range from 61 to 77, indicating intermediate weathering conditions. The exception is sample HOR27 that has a CIA value of 55, typical of unweathered crystalline rocks of granodioritic composition (Fig. 3a; Table 2; Nesbitt and Young 1989). In the ACNK diagram the samples display a general weathering trend, that starts parallel to the A-CN boundary and to the weathering path of the upper continental crust (UCC), but shows deviation toward the K apex for samples with the highest CIA, indicating K_2O enrichment comparing to UCC value (McLennan et al. 2006; Table 2). Such behavior is in accordance to XRD mineralogical and petrographical data. Comparing to data from Río Seco de los Castaños (Manassero et al. 2009) it is evident that both units have the same range of CIA variation, and similar weathering trends, although La Horqueta Formation show higher K_2O enrichment (Fig. 3a).

Weathering effects could also be detected analyzing Th/U ratios and their variation regarding Th concentrations (McLennan et al. 1993), although attempts performed on Ordovician clastic units of the San Rafael block have led to uncertain results (Abre 2007; Abre et al. this volume). Compared to UCC averages of Th (10.7 ppm) and U (2.8 ppm) according to McLennan et al. (2006), most of the samples from La Horqueta Formation (including HOR27) are enriched in Th concentrations (14 ppm on average), and show similar to enriched U concentrations (4 ppm is the average of the unit as well as the U content of HOR27). Nonetheless, the Th/U ratios are in general around 3.5–4, which is typical for unrecycled samples derived from the UCC, although a few samples have higher Th/U ratios (maximum value 6.02) indicating weathering (Fig. 3b). Sample HOR27 has a Th/U ratio of 3.99, therefore clustering along with all samples. The Río Seco de los Castaños Formation shows a narrower spread of data, since values lower than the UCC are not present (Fig. 3b).

Recycling: Resistant heavy minerals tend to be concentrated during reworking, and this effect could be deciphered by analyzing the content of elements typically carried on such heavy minerals. The Zr/Sc ratios of La Horqueta Formation range between 5.2 and 36.6, indicating that the detrital components were not recycled (Fig. 3c). Sample HOR27, with a Zr/Sc ratio of 29.31 shows the same tendency. Noteworthy are those samples with Zr/Sc ratios lower than the UCC average (14; McLennan et al. 2006), which is a response of Sc concentrations above and Zr lower than UCC average (13.6 ppm and 190 ppm, respectively; see Table 3), indicating a derivation from a source less evolved than the average UCC. The same was deduced for Río Seco de los Castaños Formation, since its narrower range of values indicate a depleted source composition and recycling was even less important comparing to La Horqueta Formation (Fig. 3c; Manassero et al. 2009).

Source composition: The average composition of the source rocks (s) could be determined through REE patterns, the character of the Eu anomaly and the content of certain trace elements which tends to be either concentrated in silicic (such as La and Th) or mafic (Sc, Cr, Co) rocks (Taylor and McLennan 1985).

The Th/Sc ratios of La Horqueta Formation range from 0.50 to 1.36 (average 0.90). Those samples with Th/Sc ratios around average UCC (0.79; McLennan et al. 2006) are explained as derived from a felsic source with a composition similar

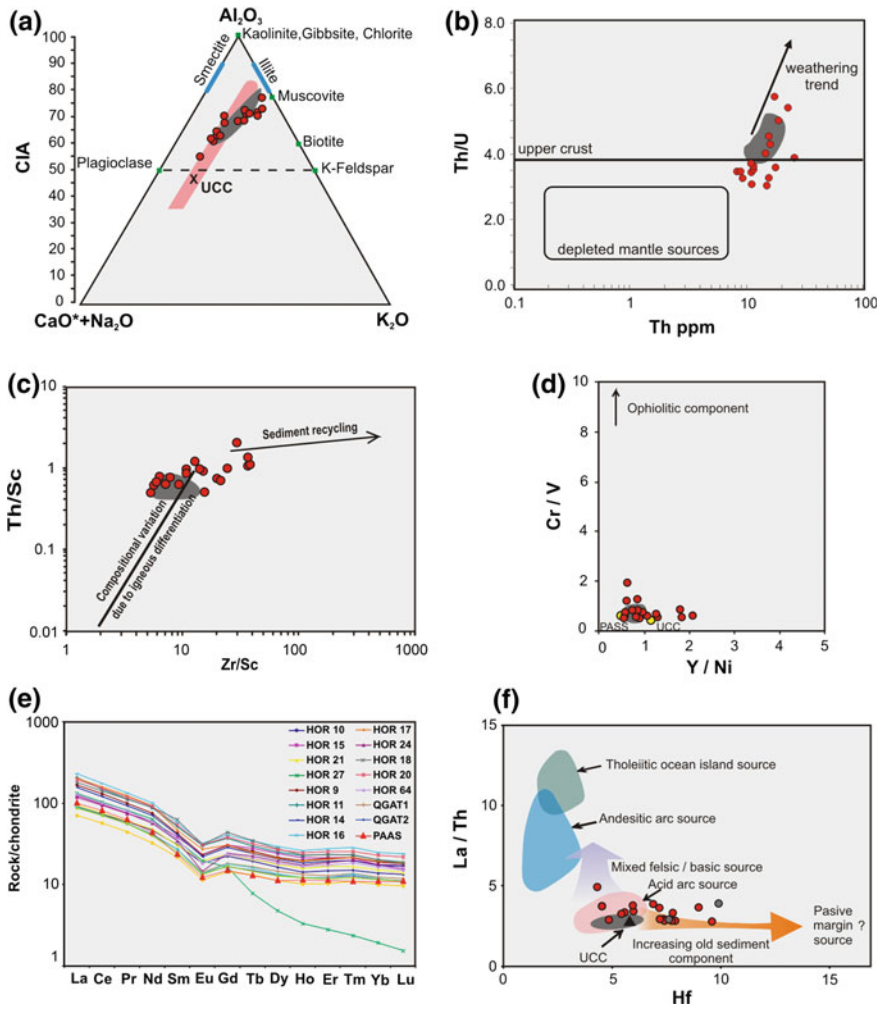

Fig. 3 **a** In the A-CN-K display La Horqueta Formation plot along a *vertical array* parallel to the expected weathering trend (field of *vertical lines*) for average *upper* crustal rocks; UCC values according to Taylor and McLennan (1985). **b** Th/U versus Th based on McLennan et al. (1993). **c** Th/Sc versus Zr/Sc display (McLennan et al. 2003): the ratios are typical of sedimentary rocks derived from unrecycled *upper* continental crust with a minor input of more depleted source composition. **d** The Y/Ni and Cr/V ratios are used to discriminate the input of a mafic source (McLennan et al. 1993). UCC values according to McLennan et al. (2006), while PAAS is following Taylor and McLennan (1985). **e** Chondrite normalized REE patterns; *PAAS* post-Archean Australian shales pattern (Nance and Taylor 1976) is draw for comparison. $Eu_N/Eu^* = Eu_N/(0.67Sm_N + 0.33Tb_N)$. **f** La/Th versus Hf after McLennan et al. (1980). For comparison range of variation of geochemical proxies of Río Seco de los Castaños Formation are shown as *gray* areas

to average UCC, with low Th/Sc ratios could have been derived from a depleted source (Fig. 3c, where it is clear the similarity to Río Seco de los Castaños Formation). La/Th ratios between 2.78 and 4.93 support felsic source rocks composition (Fig. 3f), as it was deduced for Río Seco de los Castaños Formation, although the latter display a narrower range of values ruling out any recycling (Manassero et al. 2009). Cr/V and Y/Ni ratios are between average values for UCC and Post-Archean Australian Shales (PAAS), as it is shown in Fig. 3d (see again similarities to Río Seco de los Castaños Formation; Manassero et al. 2009). The exception is sample HOR15 that display a Cr/V ratio of 2.0 due to Cr enrichment compared to UCC average of 83 ppm (McLennan et al. 2006), which along with Zr enrichment and scarce effects of recycling could indicate the presence of Cr-rich resistant heavy minerals such as first-cycle spinel that had been found in several sedimentary sequences of the San Rafael block (e.g., Abre et al. 2009, 2011). Although an ophiolitic source can be neglected, most of the samples show contents of Sc (up to 31 ppm), Cr (up to 231 ppm), and V (up to 219 ppm) above average UCC, indicating the influence of a less-evolved source.

The REE contents of La Horqueta Formation are enriched compared with PAAS, although the chondrite normalized REE patterns are parallel (Fig. 3e). The negative Eu anomaly (Eu_N/Eu^* of 0.66 on average) typical for detrital rocks derived from UCC is present. Noteworthy is the REE pattern of sample HOR27, which is parallel to PAAS regarding Light-REE, but shows extremely low concentrations of Heavy-REE; additionally, the Eu anomaly is the less negative of all samples analyzed (0.82; Table 5). Río Seco de los Castaños Formation also shows REE patterns parallel to PAAS with certain enrichment particularly regarding Heavy-REE and a negative Eu anomaly of 0.68 on average (Manassero et al. 2009), resulting therefore very similar to La Horqueta Formation, suggesting similar source composition.

The geochemical composition of sample HOR27 is not easily explained, since in summary, it shows CIA values typical for unweathered granodioritic rocks but a REE pattern that does not match such igneous compositions neither any other; therefore, laboratory errors cannot be rejected.

4 Isotope Geochemistry

Sm–Nd: Seven samples from La Horqueta Formation were analyzed using the Sm–Nd system and data are presented on Table 6. ε_{Nd} (t = 420 Ma) values range from −1.49 to −6.53, the $f_{Sm/Nd}$ are between −0.35 and −0.43, while the T^1_{DM} (average crustal residence age calculated following DePaolo 1981) range from 1.17 to 1.50 Ga and T^2_{DM} (calculated following DePaolo et al. 1991) ranges from 1.28 to 1.66 Ga. These data indicate that the average Nd isotopic signatures of the source rocks are rather a mix of both, an old upper crust and an arc component, and opposite to Río Seco de los Castaños Formation, fractionation is absent (Fig. 4a).

The εNd values are within the range of variation of data from the Cerro La Ventana Formation (Fig. 3b), which is part of the basement of the Cuyania terrane

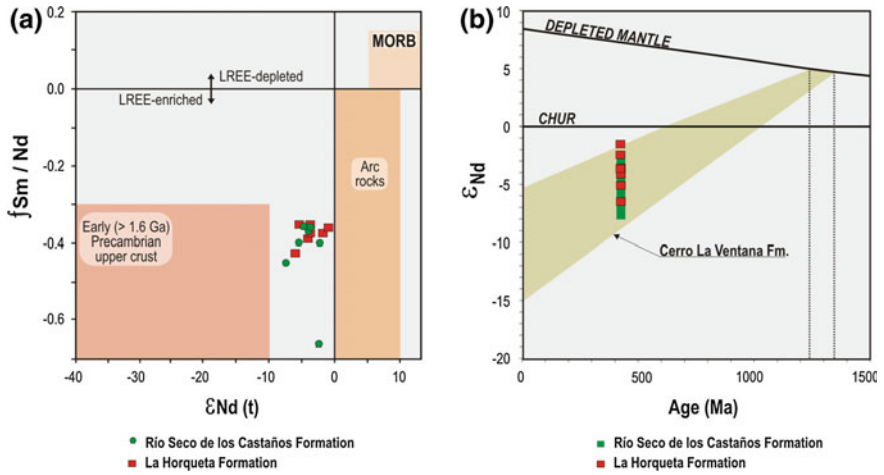

Fig. 4 **a** $f_{Sm/Nd}$ versus $\varepsilon_{Nd(t)}$ and **b** ε_{Nd} versus age. The range of Cerro La Ventana Formation Nd data (Cingolani et al. 2005b) and of Río Seco de los Castaños Formation are drawn for comparison. *CHUR* Chondritic Uniform Reservoir

outcropping within the San Rafael block (data from Cingolani et al. 2005b; Cingolani et al. this volume); The T_{DM} ages are comparable to those from Mesoproterozoic basement rocks of the Cuyania terrane studied by Kay et al. (1996) and summarized in Cingolani et al. (this volume) consistent with derivation from the nearest Grenvillian-age crustal source such as Cerro La Ventana Formation, exposed in the Ponón Trehué area. Furthermore, the Nd signature is similar to that of Río Seco de los Castaños Formation (Manassero et al. 2009), as well as to the Ordovician Pavón and Ponón Trehué Formations (Cingolani et al. 2003b; Abre et al. 2011). Ordovician to Silurian clastic sequences studied from the Precordillera *s.st.* (as part of the Cuyania terrane) also display the same range of εNd and T_{DM} values (Gleason et al. 2007; Abre et al. 2012).

Rb-Sr: Seven metapelites and six samples of micaschists were analyzed by Tickyj et al. (2001) and Tickyj et al. (this volume). The recalculated age obtained using an Isoplot/Ex Model 3 (Ludwig 2008) is 372.8 ± 8.1 Ma, initial $^{87}Sr/^{86}Sr$: 0.7164 ± 0.0012 and MSWD 8.4. The Rb-Sr data indicate that the low-grade metamorphism and folding events of La Horqueta Formation are Devonian in age. Furthermore, the age obtained agree with previous K-Ar ages reported by Linares and González (1990). The same methodology applied to Río Seco de los Castaños Formation indicate a very low-grade metamorphic age of 336 ± 23 Ma (Lower Carboniferous, Cingolani and Varela 2008). This is younger than the Rb-Sr metamorphic age of La Horqueta Formation, although both are probably linked to the final Chanic tectonic phase that occurred as a response to the accretion of Chilenia terrane at western proto-Andean Gondwana margin (Ramos et al. 1984).

5 Provenance Discussion

Geochemical analyses and particularly the Th/Sc and La/Th ratios, REE patterns and Eu anomalies indicate a derivation from a felsic source with a composition similar to average UCC, although Th/Sc and Zr/Sc ratios lower than the UCC average, along with Sc, Cr, and V concentrations suggest a provenance from source rocks slightly less evolved than the average upper continental crust. Similar conclusions were found for Río Seco de los Castaños Formation (Manassero et al. 2009) as well as for the Ordovician sequences of the San Rafael Block (Cingolani et al. 2003b; Abre et al. 2011). The agreement observed when comparing with the

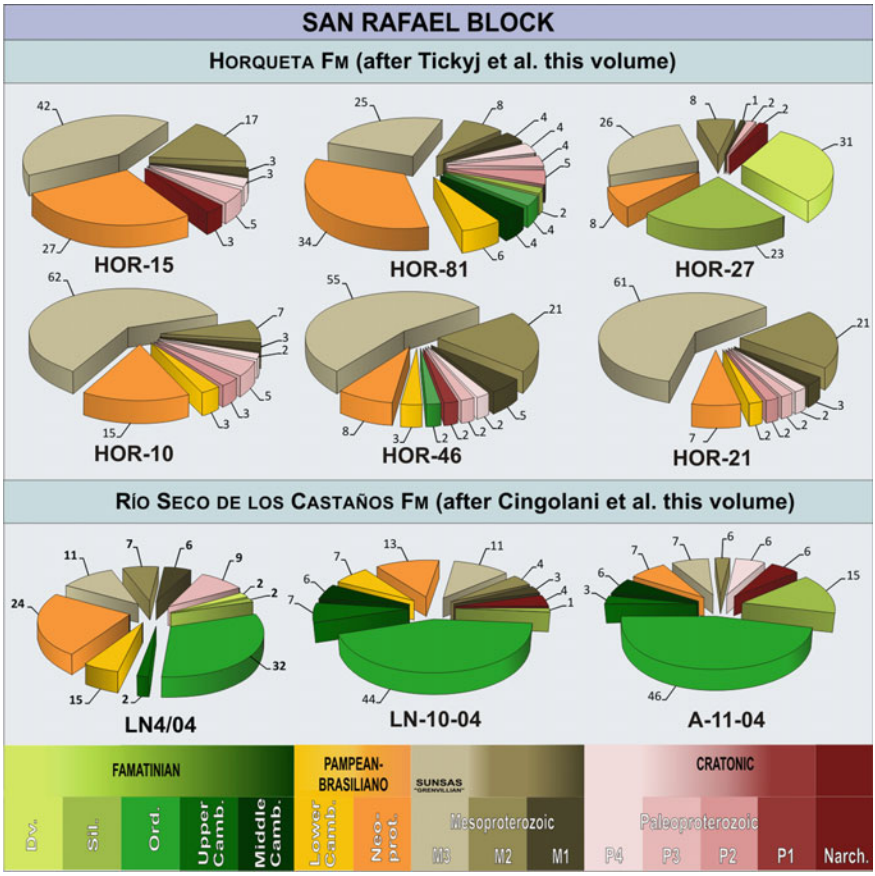

Fig. 5 Comparative U-Pb ages of the detrital zircons represented in percentage "pie diagrams" for La Horqueta and Río Seco de los Castaños Formations. Different colors are from recognized South American orogenic cycles: Archean to Paleoproterozoic; Mesoproterozoic, Brasiliano (Neoproterozoic–Early Cambrian), and Famatinian (Middle Cambrian–Devonian)

Sm–Nd signature of the Mesoproterozoic basement (Cerro La Ventana Formation) give further provenance constraints.

Zircon age patterns for La Horqueta Formation indicate four main populations, which in order of abundance correspond to the Mesoproterozoic (Grenvillian cycle), Neoproterozoic (Pampean–Brasiliano cycle), Paleoproterozoic and Upper Cambrian–Devonian (Famatinian cycle). A main derivation from the Mesoproterozoic basement of the San Rafael Block and Pampia terrane is supported, as well as a detrital input from the Río de la Plata craton and the Famatinian belt. Sample HOR27 shows however a different pattern, with a dominance of Famatinian grains, followed in abundance by the Mesoproterozoic population, the Neoproterozoic, the Paleoproterozoic and showing a few Neoarchean detrital zircon grains; it also comprises the younger detrital zircons found within the unit (ca. 0.4 Ga; Cingolani et al. 2008; Tickyj et al. this volume).

These age patterns are rather different comparing with Río Seco de los Castaños Formation which shows a dominance of Famatinian and Pampean–Brasiliano detrital zircons and lower amounts of Mesoproterozoic grains (Fig. 5). Such differences in age patterns indicate that the source rocks providing detritus to both basins were not the same.

6 Conclusions

(a) CIA values of La Horqueta Formation indicate intermediate weathering conditions, and samples with the highest CIA are enriched in K_2O comparing to UCC; some Th/U ratios support this. Zr/Sc ratios point to mainly unrecycled detritus.
(b) Th/Sc, La/Th, and Th/U ratios, REE patterns, and negative Eu anomalies are typical for detrital rocks derived from unrecycled UCC. However, Sc, Cr, and V concentrations along with low Th/Sc ratios suggest a provenance from source rocks slightly less evolved than the average upper continental crust. Sources compositions are similar to that of Río Seco de los Castaños Formation.
(c) The εNd values are within the range of variation of data from the Mesoproterozoic Cerro La Ventana Formation, which is part of the basement of the Cuyania terrane outcropping within the San Rafael Block. These isotopic data are also similar to that of the Río Seco de los Castaños Formation.
(d) Detrital zircon age patterns indicate a provenance from Mesoproterozoic (Grenvillian), Pampean–Brasiliano, and Famatinian cycles, in order of abundance.
(e) Comparison with Río Seco de los Castaños Formation indicate similar source composition based on geochemical proxies but the age of such rocks are different, according to detrital zircon age patterns. The main difference is that the Río Seco de los Castaños Formation contains larger proportion of Ordovician zircon grains while the La Horqueta Formation contains few Ordovician zircon ones and much more Grenville-aged zircons.

Acknowledgements This research was partially financed by CONICET (Grants PIPs 647; 199). We are grateful to Dr. Hugo Tickyj for field work assistance and to Dr. Héctor Ostera for several discussions and comments during revision of the manuscript.

References

Abre P (2007) Provenance of Ordovician to Silurian clastic rocks of the Argentinean Precordillera and its geotectonic implications. Ph.D. Thesis. University of Johannesburg, South Africa. UJ free web access

Abre P, Cingolani C, Zimmermann U, Cairncross B (2009) Detrital chromian spinels from Upper Ordovician deposits in the Precordillera terrane, Argentine: a mafic crust input. J S Am Earth Sci Spec Issue Mafic Ultramafic Complexes S Am Caribb 28:407–418

Abre P, Cingolani C, Zimmermann U, Cairncross B, Chemale Jr F (2011) Provenance of Ordovician clastic sequences of the San Rafael Block (Central Argentina), with emphasis on the Ponón Trehué Formation. Gondwana Res 19(1):275–290

Abre P, Cingolani C, Cairncross B, Chemale Jr F (2012) Siliciclastic Ordovician to Silurian units of the Argentine Precordillera: constraints on provenance and tectonic setting in the Proto-Andean margin of Gondwana. J S Am Earth Sci 40:1–22

Abre P, Cingolani CA, Manassero MJ (this volume). The Pavón Formation as the Upper Ordovician unit developed in a turbidite sand-rich ramp. San Rafael Block, Mendoza, Argentina. In: Cingolani C (ed) Pre-Carboniferous evolution of the San Rafael Block, Argentina. Implications in the SW Gondwana margin Springer, Berlin

Cingolani CA, Basei MAS, Llambías EJ, Varela R, Chemale Jr F, Siga Jr O, Abre P (2003a) The Rodeo Bordalesa Tonalite, San Rafael Block (Argentina): Geochemical and isotopic age constraints. 10° Congreso Geológico Chileno, Concepción, Octubre 2003, p 10 (Versión CD Rom)

Cingolani C, Manassero M, Abre P (2003b) Composition, provenance and tectonic setting of Ordovician siliciclastic rocks in the San Rafael Block: Southern extension of the Precordillera crustal fragment, Argentina. J S Am Earth Sci Spec Issue Pacific Gondwana Margin 16:91–106

Cingolani C, Varela R, Abre P (2005a) Geocronología Rb-Sr del Stock de Agua de la Chilena: Magmatismo Pérmico del Bloque de San Rafael, Mendoza. XVI Congreso Geológico Argentino, La Plata Actas en CD

Cingolani CA, Llambías EJ, Basei MAS, Varela R, Chemale Jr F, Abre P (2005b) Grenvillian and Famatinian-age igneous events in the San Rafael Block, Mendoza Province, Argentina: geochemical and isotopic constraints. In: Gondwana 12 Conference, Abstracts, p 102

Cingolani CA, Varela, R (2008) The Rb-Sr low-grade metamorphism age of the Paleozoic Río Seco de los Castaños Formation, San Rafael Block, Mendoza, Argentina. VI South American Symposium on Isotope Geology, Actas, p 4. Bariloche

Cingolani CA, Tickyj H, Chemale Jr F (2008) Procedencia sedimentaria de la Formación La Horqueta, Bloque de San Rafael (Argentina): primeras edades U-Pb en circones detríticos. XVII Congreso Geológico Argentino, San Salvador de Jujuy 3:998–999

Cingolani CA, Uriz NJ, Abre P, Manassero MJ, Basei MAS (this volume) Silurian-Devonian land-sea interaction within the San Rafael Block, Argentina: Provenance of the Río Seco de los Castaños Formation. In: Cingolani C (ed) Pre-Carboniferous evolution of the San Rafael Block, Argentina. Implications in the SW Gondwana margin Springer, Berlin

Criado Roqué P (1972) Bloque de San Rafael. In: Leanza AF (ed) Geología Regional Argentina. Academia Nacional de Ciencias, Córdoba, pp 283–295

Criado Roqué P, Ibáñez G (1979) Provincia geológica Sanrafaelino-Pampeana. In: Turner JC (ed) Segundo Simposio de Geología Regional Argentina, vol I. Academia Nacional de Ciencias, Córdoba, pp 837–869

Cuerda AJ, Cingolani CA (1998) El Ordovícico de la región del Cerro Bola en el Bloque de San Rafael, Mendoza: sus faunas graptolíticas. Ameghiniana 35(4):427–448

DePaolo DJ, Wasserburg GJ (1976) Nd isotopic variations and petrogenetic models. Geophys Res Lett 3:249–252

DePaolo DJ (1981) Neodymium isotopes in the Colorado front range and crust-mantle evolution in the Proterozoic. Nature 291:193–196

DePaolo DJ, Linn AM, Schubert G (1991) The continental crustal age distribution, methods of determining mantle separation ages from Sm-Nd isotopic data and application to the southwestern United States. J Geophys Res 96:2071–2088

Dessanti RN (1956) Descripción Geológica de la Hoja 27c-Cerro Diamante (Provincia de Mendoza). Dirección Nacional de Minería, Boletín 85:79. Buenos Aires

Gleason JD, Finney SC, Peralta SH, Gehrels GE, Marsaglia KM (2007) Zircon and whole-rock Nd–Pb isotopic provenance of Middle and Upper Ordovician siliciclastic rocks, Argentine Precordillera. Sedimentology 54:107–136

González Díaz EF (1981) Nuevos argumentos a favor del desdoblamiento de la denominada "Serie de La Horqueta" del Bloque de San Rafael, provincia de Mendoza. Congreso Geológico Argentino, No 7, Actas 3:241–256. San Luis, Argentina

Kay SM, Orrell S, Abruzzi JM (1996) Zircon and whole rock Nd–Pb isotopic evidence for a Grenville age and a Laurentian origin for the basement of the Precordillera in Argentina. J Geol 104:637–648

Linares E, González RR (1990) Catálogo de edades radimétricas de la República Argentina, años 1957–1987. Serie B (Didáctica y Complementaria) 19. Asociación Geológica Argentina, Buenos Aires, p 630

Ludwig KR (2008) User's Manual for Isoplot 3.6. A geochronological toolkit for Microsoft Excel. In: Berkeley Geochronology Center, Special Publication No 4. Berkeley, USA, p 77

Manassero M, Cingolani C, Abre P (2009) A Silurian-Devonian marine platform-deltaic system in the San Rafael block, argentine Precordillera-Cuyania terrane: lithofacies and provenance. In: Königshof P (ed) Devonian change: case studies in palaeogeography and palaeoecology. The Geological Society, London, Special Publications, vol 314, pp 215–240

McLennan SM, Nance WB, Taylor SR (1980) Rare earth element-thorium correlations in sedimentary rocks, and the composition of the continental crust. Geochim Cosmochim Acta 44:1833–1839

McLennan SM, Hemming S, McDaniel DK, Hanson GN (1993) Geochemical approaches to sedimentation, provenance, and tectonics. In: Johnsson MJ, Basu A (eds) Processes controlling the composition of clastic sediments: Geological Society of America, Special Paper, vol 284, pp 21–40

McLennan SM, Bock B, Hemming SR, Hurowitz JA, Lev SM, McDaniel DK (2003) The roles of provenance and sedimentary processes in the geochemistry of sedimentary rocks. In: Lentz DR (ed) Geochemistry of sediments and sedimentary rocks: evolutionary considerations to minerals deposit-forming environments. GeoText, vol 4. Geological Association of Canada, pp 7–38

McLennan SM, Taylor SR, Hemming SR (2006) Composition, differentiation, and evolution of continental crust: constraints from sedimentary rocks and heat flow. In: Brown M, Rushmer T (eds) Evolution and differentiation of the continental crust. Cambridge, p 377

Nance WB, Taylor SR (1976) Rare earth element patterns and crustal evolution. Australian post-Archean sedimentary rocks. Geochimica et Cosmochimica Acta 40:1539–1551

Nesbitt HW, Young GM (1982) Early Proterozoic climates and plate motions inferred from major element chemistry of lutites. Nature 199:715–717

Nesbitt HW, Young GM (1989) Formation and diagenesis of weathering profiles. J Geol 97:129–147

Patchett PJ, Ruiz J (1987) Nd isotopic ages of crust formation and metamorphism in the Precambrian of eastern and southern Mexico. Contrib Miner Petrol 96:523–528

Ramos V, Jordan TE, Allmendinger RW, Kay SM, Cortés JM, Palma MA (1984) Chilenia: un terreno alóctono en la evolución paleozoica de los Andes Centrales. 9º Congreso Geológico Argentino (Bariloche). Actas 2:84–106. Buenos Aires

Taylor SR, McLennan SM (1985) The continental crust. Its Composition and Evolution, Blackwell, London 312 pp

Tickyj H, Cingolani CA, Varela R, Chemale Jr F (2001) Rb-Sr ages from La Horqueta Formation, San Rafael Block, Argentina. III South American Symposium on Isotope Geology. Extended Abstracts, pp 628–631. Pucón. Chile

Tickyj H, Cingolani CA, Varela R, Chemale Jr F (this volume) Low-grade metamorphic conditions and isotopic age constraints of the La Horqueta pre-Carboniferous sequence, Argentinian San Rafael Block. In: Cingolani C (ed) Pre-Carboniferous evolution of the San Rafael Block, Argentina. Implications in the SW Gondwana margin. Springer, Berlin